ARTICLE

Radiative Cooling: Lattice Quantization and Surface Emissivity in Thin Coatings

Chetan N. Suryawanshi and Chhiu-Tsu Lin*

Department of Chemistry and Biochemistry, Northern Illinois University, DeKalb, Illinois 60115

ABSTRACT Nanodiamond powder (NDP), multiwall carbon nanotube (MWCNT), and carbon black (CB) were dispersed in an acrylate (AC) emulsion to form composite materials. These materials were coated on aluminum panels (alloy 3003) to give thin coatings. The active phonons of the nanomaterials were designed to act as a cooling fan, termed "molecular fan (MF)". The order of lattice quantization, as investigated by Raman spectroscopy, is MWCNT > CB ≫ NDP. The enhanced surface emissivity of the MF coating (as observed by IR imaging) is well-correlated to lattice quantization, resulting in a better cooling performance by the MWCNT−AC composite. MF coatings with different concentrations (0%, 0.4%, 0.7%, and 1%) of MWCNT were prepared. The equilibrium temperature lowering of the coated panel was observed with an increase in the loading of CNTs and was measured as 17 °C for 1% loading of MWCNT. This was attributed to an increased density of active phonons in the MF coating.

KEYWORDS: carbon nanotube • emissivity • thermal management • nanodiamond • composite coating

INTRODUCTION

Thermal management is important in the electronic (high-power, high-speed, and high-density devices) and optical (high-intensity light-emitting devices) industries. Conventional techniques usually involve (a) conduction to transfer heat from the device to the heat sink and (b) forced convection (by means of mechanical fans) to cool the heat sinks. However, these techniques require additional components, such as mechanical fans and/or a power supply, that are not desirable. Novel techniques like phase-transfer cooling (1) and microscale ionic "winds" (2) have been reported but are expensive. As electronic devices become miniaturized, radiative cooling should be very effective because the radiation transfer of energy requires no additional space and, more importantly, is independent of the surrounding conditions. Few studies have been reported for radiative cooling (3−5), including the use of inorganic pigments (4, 5).

Carbon-based materials (especially diamond) have exceptionally high thermal conductivity (κ) (6). Diamond, because of strong covalent bonding (sp^3) with the crystal, is known to have among the highest thermal conductivities (7) in solids. Graphite, the common form of carbon, is also known to have a high thermal conductivity (8), though not on the order of diamond. The discovery of nanotubes in 1991 (9) and their particular nanotubular structure has drawn interest partly because of their unique electronic and thermal properties. A carbon nanotube (CNT) is basically a graphene sheet rolled into a tubular structure on the nanometer scale, with the length being on the order of micrometers. Because of the large free path available to phonons in the stiff sp^2 network of CNT walls, CNTs have been reported to have exceptionally high thermal conductivity (10−12) and are considered second to diamond. Simulation studies have predicted κ values as high as 6600 W/mK (10) for a single-walled nanotube (SWNT). Thermal measurements on a multiwall carbon nanotube (MWCNT) have given κ values from 3000 W/mK (for an individual MWCNT (11)) to 200 W/mK (for a MWCNT array (12)).

In the past decade, various researchers have reported the use of CNT coatings in thermal management. Most of these techniques involve growth of CNT and CNT arrays (13−15) directly on the metal surface/substrate. Although growth mechanisms and several production methods have been extensively studied, the direct growth process has its limitation. The growth process involves chemical vapor deposition, which is expensive and usually requires high-temperature conditions. On the other hand, composite materials of CNTs with organic matrixes offer flexibility, cheaper alternatives, and better processing options. Different binders/resins have been investigated for improvement in thermal conductivity (16−20), but none on the basis of surface emissivity.

Recently, we reported coatings [termed molecular fan (MF)] for radiative cooling (21, 22). In this paper, we extend our work to formulate and process a coating having strong surface emissivity for effective heat dissipation. The coating composite was formulated with well-dispersed carbon materials (including carbon black, CNT, and nanodiamond powder) in an acrylate (AC) emulsion. The effective radiative cooling with enhanced surface emissivity is correlated and attributed to the lattice quantization of active phonons assembled on the coating surfaces.

EXPERIMENTAL SECTION

Suspensions. Carbon black (CB; 98.5% pure, primary particle size ~20 nm), multiwall carbon nanotube (MWCNT; 98.5% pure, OD = 10−30 nm), and nanodiamond powder (NDP; 95% pure, ~5 nm) were obtained from Akzo Nobel, Applied Nano-

* E-mail: ctlin@niu.edu.

Received for review March 24, 2009 and accepted May 14, 2009

DOI: 10.1021/am900200r

Published on Web 05/27/2009

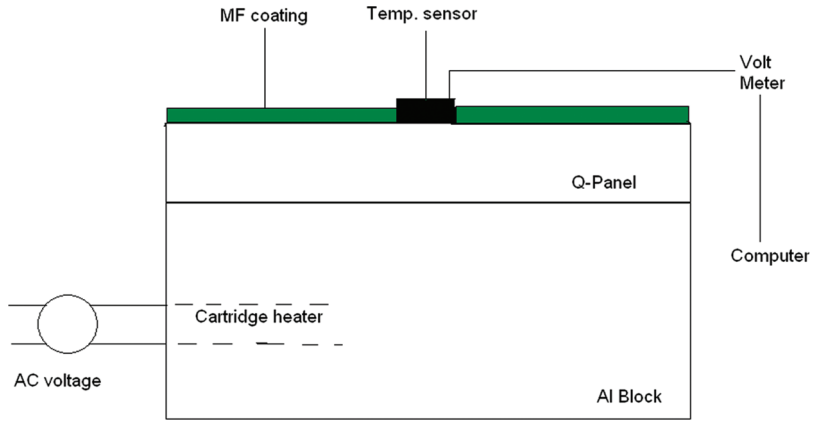

FIGURE 1. Schematic of the temperature-monitoring system.

technologies, and Maple Canada Group, respectively. Fluorosurfactant Zonyl FS-510 and a poly(tetraflouroethylene) (PTFE) dispersion were obtained from DuPont and Shamrock, respectively. Suspensions were prepared by dispersion of the carbon materials in Milli-Q water containing 0.5 wt % FS-510 and 2.5 wt % PTFE and sonication of the solution for 30 s at a power of 10 W using a Fisher Scientific sonic dismembrator (23 kHz). Under these dispersion conditions, it was noted that the composite had good dispersion up to about 2 % of CB, MWCNT, and NDP. The molecular fan (MF) coating formulation and the coated panel were inspected visually for a smooth coating film.

Composites. Suspensions were ground with steel beads with an acrylic emulsion for 2 h. Propylene glycol butyl ether was added as the cosolvent. A trace amount of additives (surface wetting agent) was also added. Aluminum Q-panels (Al 3003) were obtained from Q-Lab. Prior to coating, the panels were cleaned with Milli-Q water and 95% ethanol. The coating was sprayed on the panel by a spray gun, followed by drying at 101 °C for 15 min, to give panels with a coating thickness of ~2 μm, as measured by a coating thickness gauge (Electromatic Equipment Co., DCN-900).

The composite coatings of AC with CB, CNT, and NDP were designated as CB–AC, CNT–AC, and NDP–AC, respectively. A panel with the above formulation, but without any carbon, was coated for comparative purposes and was designated as AC.

CHARACTERIZATION

Temperature Measurement. The heat dissipation efficiency of a molecular cooling fan was measured by a temperature-monitoring system (Figure 1). A small portion in the center of the Q-panel was uncoated to mount the temperature sensor (a piece of tape was stuck to the center portion of the panel prior to spray coating; after drying of the film, the tape was removed and the uncoated portion was cleaned by acetone).

The heat source was generated by a 30 W cartridge heater, which was controlled by a variable transformer, and attached to the MF test unit. The temperature of the MF-coated film was monitored by a temperature sensor and recorded every 30 s. The potential of the transducer is measured with a multimeter that is interfaced with a PC to record data. It was observed, as shown in Figures 6 and 8 below, that the temperature of the panels equilibrated with the surroundings after 60 min of heating. To account for a possible potential variation with ambient temperature fluctuation, an uncoated control unit was run every time when the coated panels were measured. Moreover, to ensure that there is no possible air gap created between the heat block and the MF-coated panel, a pressure mechanism (~1 kg) was used to press the MF panel to the heating block.

Raman Spectroscopy. Raman data were collected on a Renishaw spectrometer (system 2000). A He–Ne laser (633 nm) was used as the excitation source. A continuous grating scan was employed with two accumulations, and the range was from 100 to 3500 cm^{-1}.

FTIR Spectroscopy. An ATI Mattson Genesis Series FTIR was used for IR characterization of the coated panels. The panels were used in attenuated total reflectance (ATR) mode. A total of 16 scans were recorded, and the range was from 650 to 4000 cm^{-1}.

IR Imaging. The IR images of the panel were taken with an Irisys universal thermal imager, type IRI 1011.

RESULTS AND DISCUSSION

CNT Suspension. The dispersion of carbon materials in aqueous systems is limited because of their strong hydrophobic character. For nanotubes, there is the additional problem of formation of ropes (due to van der Waals interaction along the length of the tube) and entanglement of ropes, which results in immediate phase separation of CNT. In NDP, the primary particles typically form aggregates and agglomerates, which settle down in water.

The requirement for preparing a stable suspension is (a) to break down the agglomerates (in the case of NDP)/entanglement of ropes (in the case of CNT) by force and (b) prevent them for reaggregating. Sonication is an effective technique for this purpose. Sonication, in a nonelastic medium like water, results in the formation of cavitation "bubbles". These bubbles grow in size until they implode under the intense pressure difference, resulting in shock waves. The intense energy and subsequent high shear forces released because of these waves aid in breaking the CNT ropes and diamond aggregates.

Researchers have employed dispersants to obtain stable suspensions of NDP (23) and CNT (24–27). The dispersants are usually low-energy surfactants and water-soluble polymers. These help prevent reaggregation by either electrostatic or steric repulsion. Researchers have investigated

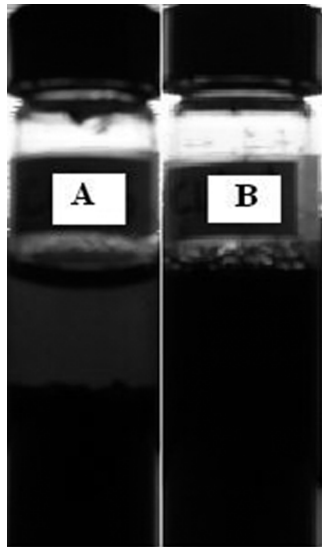

FIGURE 2. 0.2 wt % CNT suspensions in water: (A) without dispersants; (B) with dispersants.

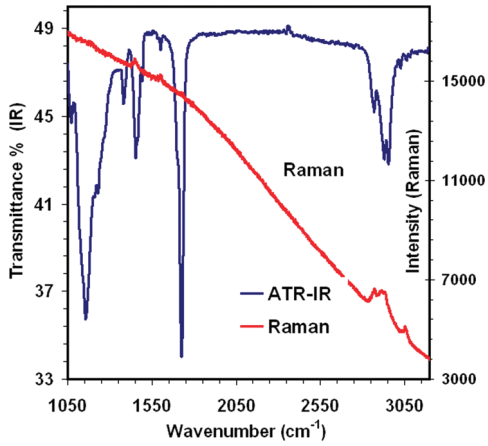

FIGURE 3. ATR-IR and Raman spectra for the AC-coated panel.

various dispersants to obtain stable CNT suspensions of different concentrations.

We report here the successful use of FS-510 (fluorosurfactant) and PTFE as dispersants. To test the effectiveness of these materials, 0.2 wt % suspensions of CNT were prepared by sonication (10 W for 10 s) and left overnight. The next day, settling was observed in the control (no dispersants, vial A), while the dispersants helped to keep the suspension stable (vial B) (Figure 2). FS-510 is a low-surface-energy surfactant that aids in the reduction of the surface energy of aqueous solution, making it more compatible with the hydrophobic surface of CNT.

Spectroscopic Data. FTIR and Raman data for the AC-coated panel are shown in Figure 3.

The AC emulsion contains an ester of styrenic acid group. The absence of the vinyl peak (~1640 cm^{-1}) indicates that the resin is polymerized. The characteristic peaks are tabulated below (Table 1). The vibration modes observed on a AC-coated panel can act as surface phonons to enhance the surface emissivity for radiative cooling of substrates.

The Raman spectra of the three carbon-based materials are shown in Figure 4. The quantized phonons at 1326 cm^{-1} (D band, transversal axial mode), 1577 cm^{-1} (G band, longitudinal mode), and 2646 cm^{-1} (first overtone of the D band) are actively seen for MWCNT (28). The same Raman bands are weakly observed for the graphene sheet in CB and barely appeared for NDP. In fact, NDP shows a broad and nonquantized Raman spectral feature. Thus, the phonon quantization is shown to follow the order of MWCNT > CB ≫ NDP. In all cases, the broad fluorescent backgrounds extended from low to high wavenumbers are clearly recorded.

Table 1. Peak Assignments in FTIR Spectra of AC Emulsion

obsd peaks (cm^{-1})	peak assignments
2960−2875	−CH stretching (sp^3)
1727	−C═O stretching
1600, 1454	aromatic C═C stretching
1386/1370	−CH bending
1162	−CO stretching

The CNT was well-dispersed in water with dispersants and then formulated with AC emulsions to form a MF coating on the aluminum panel. It is important to note that the quantization activities of lattice phonons were retained, as shown by the Raman spectra of MF-coated films (Figure 5).

The phonon modes in carbon-based materials can be exploited to form an assembly of molecular cooling structures, which was termed molecular fan (MF) (21, 22). Ideally, MF coating should have (a) enhanced emissivity on the coated

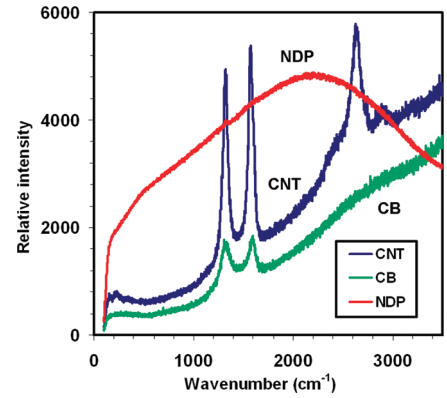

FIGURE 4. Raman spectra for the CNT (blue), NDP (red), and CB (green) used in this work.

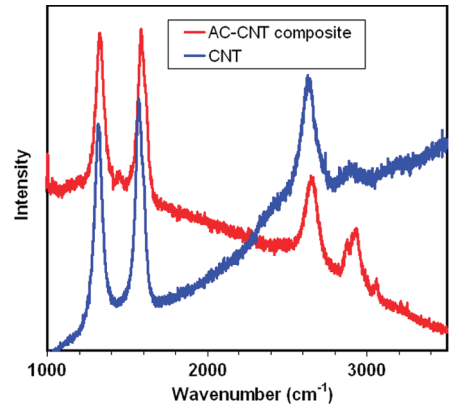

FIGURE 5. Raman spectra for the CNT and a AC−CNT composite of coated film.

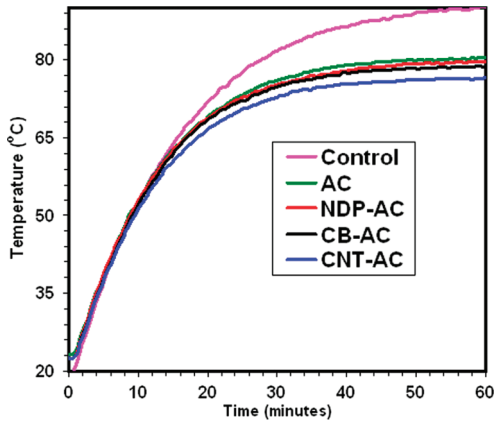

FIGURE 6. Temperature vs time curves for a bare aluminum control panel (top) and MF coatings containing 0.7 wt % of NDP, CB, and MWCNT composites and bare AC (bottom three).

surface and (b) high thermal conductivity to effectively transfer heat from the heat source (through a coated layer) to the quantized lattice motions on the coated surface. The effect of lattice quantization on the radiative surface emissivity can be viewed from a simple model that the diagonal term of the phonon thermal conductivity tensor is given by (29):

$$\kappa_{zz} = \sum C v_z^2 \tau \qquad (1)$$

$\delta\tilde{\nu}$ (uncertainty broadening of a phonon state) = 5.31 cm^{-1}/τ ps.

In eq 1, C, v, and τ are the specific heat, group velocity, and relaxation time, respectively, for a given phonon state, and the sum is over all phonon states. Therefore, the most important requirement for designing a molecular cooling fan is that the coated films should display lattice motions that are well-defined and quantized. When these quantized lattice modes are excited by the heat source at higher temperature, they will be promoted to higher quantum states and then decay to the ground-state radiatively by emitting an IR photon of energy $h\nu_i$. For MF with highly quantized phonon states, the radiative relaxation time, τ, is longer, and thus the heat dissipation efficiency, κ, should be higher because of an enhanced surface emissivity. If the lattice modes are not quantized as seen in a broad and continuous phonon band, τ is shorter and heat dissipation would be nonradiative via conduction and convection processes. The release of thermal energy, kT, nonradiatively normally leads to the self-heating of devices.

TEMPERATURE DATA

Different Types of Carbon. Figure 6 shows the temperature profile vs operation time of a MF coating on an aluminum panel, containing 0.7 wt % NDP (red curve), CB (black curve), MWCNT (blue curve), and pure AC (green curve). The pink curve is the uncoated aluminum panel as the control, with a system temperature run at 87 °C. The lowering of the equilibrium temperature for MF-coated panels as measured relative to the uncoated control panel is 8, 9, 11, and 13 °C for pure AC, NDP, CB, and MWCNT dispersed MF coatings, respectively.

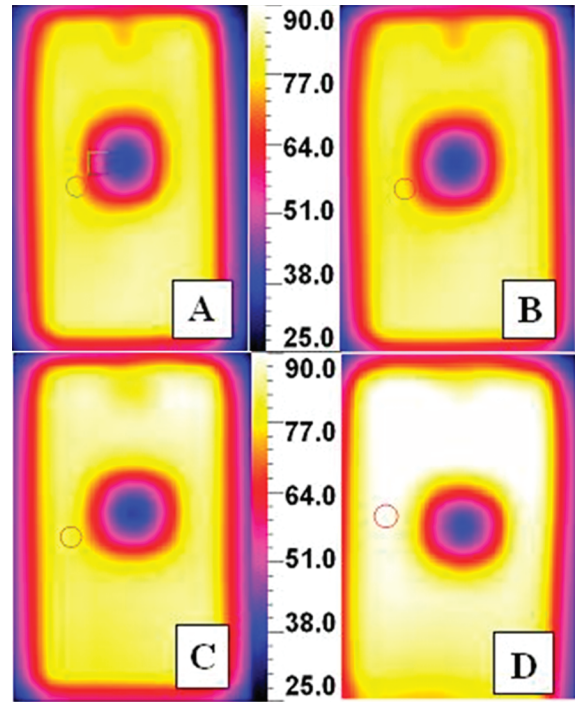

FIGURE 7. IR images for MF coatings: (A) pure AC; (B) NDP−AC; (C) CB−AC; (D) CNT−AC.

As stated earlier, the thermal conductivity of diamond is extremely large (~3000 W/mK), while that of MWNT is smaller (~200−2000 W/mK, depending on the state). Pure graphite has much smaller κ values (~40 W/mK).

If thermal conductivity, and hence conduction, is the sole factor in thr cooling performance, NDP−AC should exhibit the best results followed by CNT−AC, CB−AC, and AC. The indication that CNT−AC and CB−AC are better than NDP−AC implies that conduction is not a significant mode of cooling for the system. The results in Figure 6 seem to suggest that the surface emissivity of the MF coating may have played an important role in releasing heat from the heat source to the panel and to the surroundings radiatively.

As discussed earlier, the radiative cooling can be effective when the molecular modes and lattice motions assembled on the coated surface are quantized. From Figure 4, the lattice quantization for MWCNT is the highest, for CB moderate, and for NDP very small with a broad-band distribution. Thus, the slightly superior cooling performance of CB−AC as compared to NDP−AC can be attributed primarily to the relatively high emissivity of the coating surface, in spite of the huge difference between their thermal conductivity. The best cooling performance shown by CNT−AC can be explained by the combination of the high thermal conductivity and more significantly high surface emissivity of MWCNT. The slightly better cooling performance of NDP−AC over AC could be attributed to the high κ value of NDP.

IR Imaging. To test the hypothesis that surface emissivity plays an important role in cooling, IR imaging was employed. At a controlled heat source temperature (i.e., 90 °C in Figure 2 for the uncoated aluminum panel as the control), the radiative power of the coating film was imaged by an IR imager, as shown in Figure 7. These images are those MF panels tested in Figure 6 for (A) a pure AC emulsion coating, (B) 0.7 wt % NDP−AC, (C) 0.7 wt % CB−AC, and (D) 0.7 wt %

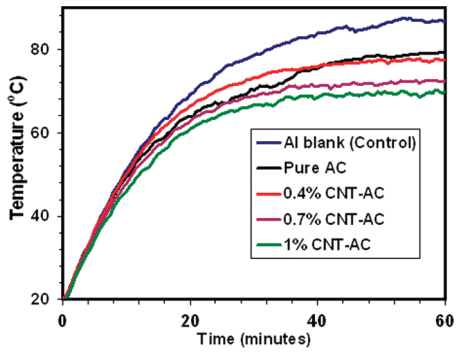

FIGURE 8. Temperature vs time curves for a bare aluminum control panel (top) and different loadings of MWCNT in MF coatings (CNT−AC).

CNT−AC. The IR image D is "hottest" or has the highest emissive surface temperature (~90 °C) that corresponds to the highly quantized lattice modes of MWCNT dispersed in a MF coating. The panel D has the lowest equilibrium substrate temperature of ~77 °C, as shown in Figure 6 (i.e., a 13 °C lowering in the equilibrium substrate temperature as compared to the control panel). The lowering of the equilibrium substrate temperature is due to radiative cooling of the MF assembly by the emission of IR photons. The IR image C displays a lesser emissive surface than image D because the lattice quantization activity of CB is lower than that of MWCNT (Figure 4).

The NDP has a high thermal conductivity but does not show any appreciable activity of lattice quantization, as indicated in Figure 4. The image B shows a surface emissivity similar to that of image A. The lowering of the equilibrium temperature by ~9 °C for panel B as compared to that by ~7 °C for panel A in Figure 7 is due to dispersion of the thermally conductive NDP in panel B.

Different Loading of CNT. The density of the lattice modes assembled on the coated MF surface and the amount of thermally conductive materials dispersed in the coating will affect the heat dissipation efficiency and subsequently the MF performances on heat sink devices. To test this concept, a set of MF coatings were applied to have the same coating thickness but a different density of the lattice modes using different amounts of MWCNT in the formulation. Figure 8 shows temperature vs time curves of MF coatings for four loading concentrations: 0% (black), 0.4% (red), 0.7% (purple) and 1% (green) by weight of MWCNT in coatings.

The blue curve in Figure 8 is the uncoated aluminum panel as the control, with a system temperature run at 87 °C. As expected, the lowering of the equilibrium temperature for MF-coated aluminum panels as measured relative to the control panel was observed. The temperature lowering is observed as 7 °C (0% or pure AC), 9 °C (0.4%), 14 °C (0.7%), and 17 °C (1%). It is worthwhile to mention that in our laboratory a radiative cooling monitor system has been constructed for the simultaneous measurement of the surface emissivity of the MF coating and the cooling efficiency of the heat source. The details of the monitor unit and its test results of MF cooling devices are in progress.

CONCLUSIONS

In summary, a high-surface-emissivity MF coating, consisting of an AC resin and carbon-based materials, has been designed, formulated, and applied on aluminum panels. The MF nanocoating, having quantized lattice motions, can act as a selective emitter and display an enhanced emissivity. The lattice quantization, surface emissivity, and hence cooling effect was observed in the order of MWCNT > CB > NDP. Increased loading of MWCNT in a MF coating gave better cooling. Using 1 wt % MWCNT, the MF coating on one side of the aluminum test panel lowers the equilibrium temperature of the heat sink by 17 °C. The radiative cooling efficiency of the MF coating has been shown to depend on the quantization of lattice and molecular vibrational modes.

REFERENCES AND NOTES

(1) Tan, F. L.; Tso, C. P. *Appl. Therm. Eng.* **2004**, *24*, 159–169.
(2) Go, D. B.; Garimella, S. V.; Fisher, T. S. *J. Appl. Phys.* **2007**, *102*, 053302-1–053302-8.
(3) Granqvist, C. G. *Appl. Opt.* **1991**, *20*, 2606–2611.
(4) Orel, B.; Klanjsek Gunde, M.; Krainer, A. *Sol. Energy* **1993**, *50*, 477–482.
(5) Nilsson, T. M. J.; Niklasson, G. A. *Sol. Energy Mater. Sol. Cells* **1995**, *37*, 93–118.
(6) Kaye, G. W. C.; Laby, T. H. *Tables of Physical and Chemical Constants*, 15th ed.; Longman: New York, 1995; p 67.
(7) Tzuk, Y.; Tal, A.; Goldring, S.; Glick, Y.; Lebiush, E.; Kaufman, G.; Lavi, R. *IEEE J. Quantum Electron.* **2004**, *40*, 262–269.
(8) Klett, J. W.; Mcmillan, A. D.; Gallego, N. C.; Walls, C. A. *J. Mater. Sci.* **2004**, *39*, 3659–3676.
(9) Ijima, S. *Nature* **1991**, *354*, 56–58.
(10) Berber, S.; Kwon, Y. K.; Tománek, D. *Phys. Rev. Lett.* **2000**, *8*, 4613–4616.
(11) Kim, P.; Shi, L.; Majumdar, A.; Mceuen, P. L. *Phys. Rev. Lett.* **2001**, *87*, 215502-1–215502-4.
(12) Yang, D. J.; Zhang, Q.; Chen, G.; Yoon, S. F.; Ahn, J.; Wang, S. G.; Zhou, Q.; Wang, Q.; Li, J. Q. *Phys. Rev. B: Condens. Matter Mater. Phys.* **2002**, *66*, 165440−1165440−6.
(13) Cho, D. B.; Suhr, J.; Koratkar, N. A. *J. Intell. Mater. Syst. Struct.* **2006**, *17*, 209–216.
(14) Kilparick, S. J.; Geil, B. R.; Ibitayo, D.; Zheleva, T. S.; Ervin, M. H.; Wickenden, A. E.; Ajayan, P. M.; Talapatra, S.; Li, X.; Ci, L.; Kar, S.; Soldano, C.; Vispute, R. D.; Hullavarad, S. S.; Venkatasan, T. *25th Army Science Conference*, 2006; pp 1−6.
(15) Xu, J.; Fisher, T. S. *Int. J. Heat Mass Transfer* **2006**, *49*, 1658–1666.
(16) Sample, J. L.; Rebello, K. J.; Saffarian, H.; Osiander, R. *InterSoc. Conf. Therm. Phenom.* **2004**, *1*, 297–301.
(17) Liu, C. H.; Huang, H.; Wu, Y.; Fan, S. S. *Appl. Phys. Lett.* **2004**, *84*, 4248–4250.
(18) Biercuk, M. J.; Llaguno, M. C.; Radosavljevic, M.; Hyun, J. K.; Johnson, A.; Fischer, J. E. *Appl. Phys. Lett.* **2002**, *80*, 2767–2769.
(19) Caneba, G. T.; Axland, J. *J. Mineral. Mater. Charact. Eng.* **2004**, *3*, 73–80.
(20) Huang, H.; Liu, C. H.; Wu, Y.; Fan, S. S. *Adv. Mater.* **2005**, *17*, 1652–1656.
(21) Lin, C. T. Molecular Fan. U.S. Patent Appl. 11/331,492, filed 01/13/2006; PCT/US06/62703, filed 12/29/2006.
(22) Sizemore, C. A.; Recchia, M. L.; Kim, T.; Lin, C. T. Surfaces and Films. *Technical Proceedings of the 2005 NSTI Nanotechnology Conference and Trade Show*; NSTI: Cambridge, MA, 2005; Vol. 2, Chapter 5, pp 339−342.
(23) Ozawa, M.; Inaguma, M.; Takahashi, M.; Kataoka, F.; Krüger, A.; Osawa, E. *Adv. Mater.* **2007**, *19*, 1201–1206.
(24) Moore, V. C.; Strano, M. S.; Haroz, E. H.; Hauge, R. H.; Smalley, R. E. *Nano Lett.* **2003**, *3*, 1379–1382.
(25) Islam, M. F.; Rojas, E.; Bergey, D. M.; Johnson, A. T.; Yodh, A. G. *Nano Lett.* **2003**, *3*, 269–273.
(26) Bandyopadhyaya, R.; Roth, E. N.; Regev, O.; Rozen, R. Y. *Nano Lett.* **2002**, *2*, 25–28.
(27) O'Conell, M. J.; Boul, P.; Ericson, L.; Huffman, C.; Wang, Y.; Haroz, E.; Kuper, C.; Tour, J.; Ausman, K.; Smalley, R. *Chem. Phys. Lett.* **2001**, *342*, 265–271.
(28) Dresselhaus, M. S.; Dresselhaus, G.; Saito, R.; Jorio, A. *Phys. Rep.* **2005**, *409*, 47–99.
(29) Hone, J.; Whitney, M.; Piskoti, C.; Zettl, A. *Phys. Rev. B: Condens. Matter Mater. Phys.* **1999**, *59*, R2514−R2516.

AM900200R